

# FIRST INVESTIGATION OF THE CLUSTERING ENVIRONMENT OF DAMPED LYMAN $\alpha$ ABSORBERS AT $Z \simeq 4^1$

ERIC GAWISER<sup>2,3</sup>, ARTHUR M. WOLFE<sup>2,3</sup>, JASON X. PROCHASKA<sup>2,4</sup>, KENNETH M. LANZETTA<sup>2,5</sup>, NORIAKI YAHATA<sup>5</sup>, & ANDREAS QUIRRENBACH<sup>2,3</sup>

*Submitted to Astrophysical Journal*

## ABSTRACT

We report the first observations of the clustering environment of damped Lyman  $\alpha$  absorption systems at  $z \simeq 4$ . Color selection and photometric redshifts were used to select 44 candidate Lyman-break galaxies brighter than  $I_{AB} = 25.5$  from deep BRI images of the 35 arcmin<sup>2</sup> field containing the quasar BR 0951–04. Multislit spectroscopy of 35 candidate galaxies was performed and 8 of these candidates have been confirmed as  $z > 3.5$  Lyman-break galaxies. With only BRI photometry, the photometric redshifts are quite accurate for the spectroscopically confirmed galaxies but have a high rate of misclassification due to color degeneracies between Lyman-break galaxies and low-redshift ellipticals. Both of the  $z > 3.5$  galaxies found within 15" of the quasar line-of-sight appear to be causing absorption systems in the quasar spectrum. We use a battery of statistical tests to look for clustering in the redshift histogram of the  $z > 3.5$  galaxies but do not find measurable clustering of these Lyman-break galaxies with the damped Lyman  $\alpha$  absorbers. With a larger sample of galaxies, our method should determine the cross-correlation between these objects, which probes the bias and hence the mass of the damped Lyman  $\alpha$  absorbers.

*Subject headings:* galaxies: high-redshift, cosmology: observational

## 1. INTRODUCTION

Galaxy formation is one of the great unsolved problems in astrophysics. We have clear evidence that many galaxies were in place at redshifts of 3 – 4 but little knowledge of how or when they formed. Using Lyman-break imaging techniques, Steidel et al. (1996) discovered a large sample of  $z \simeq 3$  galaxies with rest-frame ultraviolet luminosities  $L_{UV} > 10L_*$  and comoving number density comparable to that of  $L_*$  galaxies today. These Lyman-break galaxies (LBGs) exhibit surprisingly strong clustering for  $z \simeq 3$ , with overdensities  $\delta\rho/\rho > 3$  and comoving correlation length  $r_0 \approx 5h^{-1}$  Mpc (Adelberger et al. 1998). In hierarchical models of structure formation such as  $\Lambda$ CDM, the LBGs will undergo significant merging and should be even more clustered, rare massive galaxies today.

The damped Lyman  $\alpha$  absorption systems (DLAs), on the other hand, are thought to be the progenitors of typical present-day galaxies (Wolfe et al. 1986; Kauffmann 1996). We therefore must learn about the mass and environment of high-redshift DLAs if we want to understand the formation of typical galaxies like the Milky Way. The damped Lyman  $\alpha$  absorbers are dense clouds of neutral hydrogen seen in absorption along the line of sight to distant quasars. They appear to be drawn from the bulk of the protogalactic mass distribution; this conclusion is supported by the agreement between the comoving mass density of neutral gas at  $z > 2$  and the mass density of visible stars in current galaxy disks (Wolfe et al. 1995). However, the total gas content cannot distinguish CDM scenarios in which DLAs are numerous low-mass protogalaxies from passive

evolution models in which the DLAs are more rarely occurring massive objects. Determining the mass of individual DLAs is also critical for testing models of galaxy formation within the CDM paradigm. This determination cannot be performed using the absorption characteristics of the DLAs, as the comoving density of DLAs cannot be determined without knowing their typical cross-sectional area. One way to distinguish among models for the DLAs is to measure the kinematics of the gas (Prochaska & Wolfe 1997, 1998; Wolfe & Prochaska 2000a,b). This paper describes an independent method which seeks to determine the mass of the DLAs by investigating the extent to which they cluster with LBGs. Since DLAs are predicted by hierarchical cosmologies to be rather weak in emission, and observation is consistent with this (Steidel et al. 1995), it may be easier to constrain their mass using large-scale structure techniques than by searching for their emission (see Wolfe 1993).

Section 2 describes the theoretical basis for our investigation of the cross-correlation of DLAs and LBGs. Imaging observations and photometric data reduction are described in §3, and our multislit spectroscopy is presented in §4. We discuss the search for emission from the DLAs themselves in §5, search for evidence of clustering with nearby LBGs in §6, and discuss our results in §7.

## 2. LARGE-SCALE STRUCTURE AT HIGH REDSHIFT

Hierarchical models of structure formation predict that the most massive galaxies tend to form in regions of unusually high density, whereas low-mass galaxies are more uniformly distributed in space. This leads to an enhance-

<sup>1</sup>Based on data obtained at the W. M. Keck Observatory which is operated as a scientific partnership among the University of California, the California Institute of Technology, and NASA and was made possible by the generous financial support of the W. M. Keck Foundation.

<sup>2</sup>Visting Astronomer, Keck Observatory

<sup>3</sup>Center for Astrophysics and Space Sciences and Department of Physics, University of California at San Diego, La Jolla, CA 92037, egawiser,awolfe,aquirrenbach@ucsd.edu

<sup>4</sup>The Observatories of the Carnegie Institute of Washington, 813 Santa Barbara Street, Pasadena, CA 91101, xavier@ociw.edu

<sup>5</sup>Department of Physics and Astronomy, State University of New York at Stony Brook, Stony Brook, NY 11794-3800, lanzetta,nyahata@sbastr.ess.sunysb.edu

ment in the clustering of high-mass galaxies, referred to as bias, since they typically form near each other in rare overdense regions. Clustering thus provides a way to probe the mass distribution of DLAs; if there is a significant overdensity of LBGs near damped Lyman  $\alpha$  absorbers it indicates that the DLAs reside in massive dark halos. If, on the other hand, the DLAs are preferentially found in regions with an underdensity of LBGs, it would argue that some environmental effect, perhaps ionizing radiation from massive stars in the LBGs (see Steidel et al. 2000), prevents the occurrence of large column densities of neutral hydrogen in overdense regions. The expected result in hierarchical cosmologies is intermediate; DLAs are predicted to be low-mass objects and should be found in both the (proto)clusters and the field with typically only a small enhancement of LBGs nearby.

While the cross-correlation of galaxies and clusters has been studied at low redshift (e.g. Mo et al. 1993), these objects can also be studied through their autocorrelation. The inevitable sparse sampling of DLAs and other absorption systems caused by only being able to detect them on the line of sight towards quasars or bright galaxies makes it very difficult to measure their autocorrelation. Hence, the cross-correlation is the best, and perhaps only, way to study the bias of DLAs. Another advantage is that the cross-correlation of DLAs and LBGs can be established without detecting emission from the galaxy causing the damped Lyman  $\alpha$  absorption.

The probability of finding an LBG in a small volume  $dV$  a distance  $r$  from a known DLA is enhanced versus the average density of LBGs,

$$dP_{LBG} = [1 + \xi_{DL}(r)]\rho_{LBG}dV, \quad (1)$$

where  $\xi_{DL}$  is the cross-correlation function of DLAs and LBGs. On scales where linear bias is a good model, the cross-correlation of any two classes of objects is determined by multiplying the dark matter correlation function  $\xi(r)$  by the product of the bias factors of each class:

$$\xi_{12}(r) = b_1 b_2 \xi(r). \quad (2)$$

The bias of a set of collapsed objects of a given mass can be determined using the extended Press-Schechter method (see Mo et al. 1996). The autocorrelation of LBGs ( $\xi_{LL}$ ) is known at  $z = 3$  (Adelberger et al. 1998) but has not yet been determined at  $z = 4$  (Steidel et al. 1999, hereafter S99), probably due to the increased difficulty of obtaining redshifts at  $z \simeq 4$ . The bias of other high-redshift objects such as quasars, radio galaxies, or Lyman  $\alpha$  emitters can also be determined using the cross-correlation function.

### 3. IMAGING AND PHOTOMETRY

We took deep BRI images of the field around the  $z = 4.37$  quasar BR 0951–04 (Storrie-Lombardi et al. 1996) with the LRIS instrument (Oke et al. 1995) at the Keck Observatory. This field was chosen because there are two DLAs along the line of sight towards BR 0951–04, at  $z = 3.86$  and  $z = 4.20$  (Storrie-Lombardi & Wolfe 2000). Table 1 lists the exposure time and final depth in each filter. Images were reduced using a mix of standard IRAF routines and customized code. The final images cover a  $5' \times 7'$  field. Photometry was performed on the R image

<sup>6</sup>Our filter set corresponds closely to their custom set except for an overall 200Å ( $\Delta z \simeq 0.2$ ) shift bluewards in B and R, allowing the approximation  $(B-R)_{AB} = (G-R)$ . Because our I filter is close to theirs in effective wavelength, our  $(R-I)_{AB}$  colors should be roughly 1.6 times their  $(R-i)$  colors.

<sup>7</sup>Available at <http://zwolfkinder.jpl.nasa.gov/~stern/homepage/bogus.html>

using SExtractor (Bertin & Arnouts 1996) and then a custom code was used to extract photometry from the final B and I images using the exact apertures selected in R. Prochaska et al. (in preparation) describe our data reduction methods in greater detail and make our photometric catalog and images public.

We modified the *GRI* color selection criteria of S99 for our Johnson-Cousins BRI filter set.<sup>6</sup> Objects located in the region of color-color space bounded by  $(B-R)_{AB} \geq 2.0$ ,  $(B-R)_{AB} \geq 1.2(R-I)_{AB} + 1.6$ , and  $(R-I)_{AB} \leq 1.0$ , have a high probability of being Lyman-break galaxies at  $z > 3.5$ . We have also used photometric redshifts (see Yashata et al. 2000) and have found at least one LBG that would have been missed using only the two-color region of S99. Almost all of the color-selected candidates are identified by the photometric redshift technique as having a high probability of being at  $3.5 < z < 4.5$ . The photometric redshift method accounts for the individual photometric uncertainties in the B, R, and I fluxes of each object and compares the object fluxes with a set of template spectra rather than a single two-color region. Carefully designed seven-color photometric redshift schemes yield a scatter of  $\Delta z = 0.2$  at these redshifts (Hogg et al. 1998). It should therefore be impossible for photometric redshift selection to create a redshift distribution as narrow as the  $\Delta z \simeq 0.04$  ( $\simeq 2000$  km/s) redshift spikes seen by Adelberger et al. (1998).

We visually inspected all candidate galaxies in our images and rejected roughly half of the initial candidates for having suspect photometry. Many of the rejected objects lied near the edge of our imaging field in regions of lower signal-to-noise. It is no surprise that such a high fraction of the initial candidates had suspect photometry, as the color selection region is sparsely populated and therefore the small fraction of low-redshift galaxies scattered into the color-selection region by photometric errors can easily comprise a large fraction of the candidates. Bright ( $I < 23$ ) objects with clearly non-stellar morphology were rejected as low-redshift interlopers, but bright stellar objects were retained in case they were new quasars or lensing-magnified LBGs; most LBGs will look similar to point sources at the resolution of our images.

### 4. SPECTROSCOPY AND REDSHIFT DETERMINATION

We performed longslit spectroscopy of two objects near BR 0951–04 and multislit spectroscopy of this field with four different slitmasks, all with 1.5" width slitlets and the 150 line/mm grating (30 Å resolution) on Keck-LRIS. Table 1 lists details of our observations. Each slitmask targeted about 15 candidate objects. The entire LRIS imaging field was covered using 2 slitmasks (termed left and right) that overlap in the region near the quasar. These masks were redesigned for the March 2000 run to eliminate slits on objects whose redshifts were already determined and to add slits on additional candidate LBGs. We used a GG495 dichroic filter to block second order light in December 1999 but decided against this in the subsequent run because wavelengths below 4950 Å can be used to check for the presence of the Lyman limit. The spectroscopic data were reduced using standard IRAF techniques called by a customized version of

the BOGUS code<sup>7</sup>. The functions *response* (halogen lamp spectrum fitting), *background* (sky subtraction) and *apall* (spectrum extraction) were performed interactively following the multislit data reduction cookbook available at <http://mamacass.ucsd.edu/people/gawiser/cookbooks.html>. Redshifts were determined interactively using a customized PGPlot routine which compared the measured spectra with templates of expected absorption (and emission) lines for LBGs (Steidel et al. 2000; Lowenthal et al. 1997) and E+A galaxies (Zabludoff et al. 1996). Gawiser et al. (in preparation) describe our spectroscopic data reduction in greater detail.

We obtained spectra of 35 candidate galaxies in the field of BR 0951–04 (see Table 2). Eight candidates turn out to be galaxies at  $z > 3.5$ , thirteen appear to be low-redshift interlopers (typically ellipticals at  $z \simeq 0.5$ ) and fourteen have inconclusive spectra. Our color-selected sample with  $I_{AB} \leq 25$  is directly comparable to the objects observed by S99. We find 0.5 candidates per sq. arcmin, twice the candidate density of S99; the difference is unlikely to be caused solely by Poisson fluctuations given that there are 19 objects in this category in Table 2. Our rate of determining redshifts for objects observed spectroscopically is comparable to S99, and the fraction of candidates identified as interlopers, i.e. at  $z < 3.5$ , is higher but very sensitive to small-number statistics at present. We will revisit this comparison once a larger sample of BRI-selected galaxies is available.

Figure 1 shows the two-color diagram of all 2254 objects with  $I_{AB} < 25.5$  detected in the field with the status of LBG candidates shown. Table 3 lists photometry and photometric redshift information on each  $z > 3.5$  galaxy with its best-fit redshift and uncertainty. The photometric redshifts based on BRI alone are impressively accurate for the confirmed high-redshift galaxies, with a dispersion of  $\sigma = 0.18$ , including three cases where  $z_{phot}$  differs from the spectroscopic redshift by only 0.01. However, adding in the catastrophic failures where  $z \simeq 0.5$  galaxies were assigned photometric redshifts  $z_{phot} \simeq 4$  would drastically increase this dispersion. Adding near-infrared (JHK) or optical Z-band photometry would be quite helpful in discriminating against these intrinsically-red low-redshift interlopers.

The increased fraction of interlopers among candidates selected primarily by photometric redshift confirms that the S99 color selection region is the most efficient place to find LBGs. However, we differ from S99 in one major respect. We do not assume that the spectra with insufficient signal-to-noise for redshift determination are drawn from the same population of objects as those with identified redshifts. Thus there is a factor of two uncertainty in the number abundance of color-selected  $z > 3.5$  galaxies, both here and in S99, caused by almost half of the candidates lacking redshift identifications. Extrapolating from the observed color distribution of LBGs at  $z = 3$ , S99 predict that roughly half of the  $z = 4$  LBGs will lie outside of the color selection region. The failure of photometric redshifts to find these LBGs implies either that this incompleteness has been overestimated or that the photometric redshift technique needs to be modified to better identify LBGs with unusual colors.

Figure 2 shows the rest-frame spectra of the confirmed  $z > 3.5$  galaxies. These spectra show the typical mix of Lyman  $\alpha$  emission (G4, G6, G7) and Lyman  $\alpha$  absorption (G1, G2, G8) as well as two vague suggestions of emission within a broad absorption trough (G3, G5). The signal-

to-noise is generally quite poor, illustrating why  $I=25$  is usually considered the limit for ground-based optical spectroscopy.

## 5. SEARCH FOR EMISSION FROM DAMPED LYMAN $\alpha$ ABSORBERS

At  $z \sim 4$ , Lyman-break galaxies found within a  $10''$  radius of the quasar may be the source of damped Lyman  $\alpha$  absorption. This radius corresponds to the maximum impact parameter ( $\sim 100$  kpc) inferred from absorption line statistics in the passive evolution model (Storrie-Lombardi & Wolfe 2000; Bunker et al. 1999). If DLAs represent formed disk galaxies as postulated by Wolfe (1997), we should be able to detect emission from up to 20% of them at  $R \leq 25$  (Maller et al. 2000). However, in hierarchical models of structure formation, a much higher fraction of DLAs are expected to be too dim and/or too close to the quasar to yield detectable emission (Haehnelt et al. 1998, 2000). Our survey hopes to differentiate between these hypotheses; if emission from DLAs is found repeatedly at large impact parameters or high luminosity it will represent a serious conflict with the predictions of hierarchical cosmology.

We performed a complete survey for possible emission from DLAs on the line of sight toward the quasar down to  $I_{AB} = 26$  at angular distances up to  $10''$ , although the PSF of the quasar hampers our survey at angles less than  $2''$  where hierarchical cosmology predicts that the emission from most DLAs will be found. We identified three objects within  $10''$  of the QSO line-of-sight that had a reasonable chance of being at high redshift (our selection criteria were less stringent in this region). One of these, G1, meets the color selection criteria but has  $I_{AB} = 25.7$  and appears to have a redshift of 3.69. Although G1 is  $10''$  from the QSO, it may be responsible for the  $z = 3.703$  absorption system seen in SiIV and CIV (Storrie-Lombardi et al. 1996). The second nearby object appears to be a low-redshift interloper, and the third has inconclusive redshift. Another color-selected galaxy, G2 at  $z = 3.81$ , lies  $15''$  ( $\simeq 200$  kpc) from the QSO and may be responsible for the  $z = 3.818$  absorption system seen in Lyman  $\alpha$  and CIV in our Keck-HIRES spectrum of BR 0951–04 (Prochaska & Wolfe 1999). It will be interesting to determine the fraction of galaxies detected in both emission and absorption as a function of distance from the quasar line-of-sight. We have not detected emission physically associated with either of the damped Lyman  $\alpha$  absorbers towards BR 0951–04 spectroscopically, but all of the models predict that a larger sample is needed before we should expect to find an LBG physically associated with a DLA.

## 6. CLUSTERING ANALYSIS

Figure 3 shows the redshift histogram of objects in the field of BR 0951–04, with a binsize of  $\Delta z = 0.05$  ( $\sim 10h^{-1}$  Mpc) chosen because most of our redshift uncertainties are smaller than this value. We chose to place the  $z = 3.86$  DLA in the center of a bin in order to maximize the chance of finding an overdensity (or underdensity) of LBGs near the DLA if one exists. However, the results described below are not altered by shifting the bin locations.

There are eight confirmed LBGs in the BR 0951–04 field, so the search for clustering is plagued by small number statistics. Before trying to determine the amplitude of a cross-correlation function, it makes sense to ask if any clustering has been observed that is inconsistent with poisson fluctuations about the expected redshift distribution

of LBGs. The expected redshift distribution refers to the multiplication of the true redshift distribution of LBGs on an average line of sight times the observational selection function. While the observational selection function can be simulated (see S99), the true redshift distribution of LBGs is unknown, so it is necessary to determine the expected redshift distribution empirically. We have not yet observed a sufficient number of LBGs to determine how our expected redshift distribution differs from that of S99, who found  $< z > = 4.13, \sigma = 0.26$ . We do expect a shift of 0.2 in redshift, so we choose to bracket the possibilities by showing three possible expected redshift distributions in Figure 3. The mean of all three is  $z = 3.9$ ; the dashed one is a gaussian with  $\sigma = 0.3$  and is considered the most likely, the dot-dashed one is a gaussian with  $\sigma = 0.2$  and is considered the narrowest possible, and the flat dotted one is the broadest possible (a uniform distribution from  $z = 3.3$  to  $z = 4.5$ ). The presence of a bin in our redshift histogram that contains three LBGs is only a weak indication of autocorrelation of the LBGs, because Poisson fluctuations of any of the three expected redshift distributions generate an appearance of clustering at least this strong over 10% of the time in our Monte Carlo simulations.<sup>8</sup> A Kolmogorov-Smirnov test of the unbinned cumulative redshift distribution versus the three expected distributions fails to find any inconsistencies at the 95% confidence level. A similar analysis of the reported redshifts of S99 indicates that the redshift histograms of all 7 of their fields are consistent with Poisson fluctuations of their expected redshift distribution.

We are interested primarily in the clustering environment of the DLAs. This allows us to select the bins known a priori to contain a DLA and to ask if a statistically significant overdensity (or deficit) of LBGs has been found there. Finding zero LBGs in the bin containing the  $z = 3.86$  DLA should occur at least 40% of the time for any of the expected redshift distributions. Finding zero LBGs in the bins containing the  $z = 4.20$  DLA or  $z = 4.37$  quasar is at least as common. Even the apparent triple coincidence of finding no LBGs in any of those bins occurs in at least 30% of our Monte Carlo simulations, so we do not have good evidence for an anticorrelation of DLAs and LBGs. Our results provide an upper limit on the amplitude of the DLA-LBG cross-correlation function, but it is not a particularly interesting upper limit, as even the observed strong autocorrelation function of  $z = 3$  LBGs would be difficult to detect with so few objects. A vast improvement in statistics will be required to measure the cross-correlation of LBGs and DLAs.

The minimum redshift uncertainty of our LBGs is  $\Delta z = 0.01$ , so correlations on comoving scales of a few Mpc and smaller can only be probed via angular clustering. While 8 LBGs and 2 DLAs are insufficient to measure the angular cross-correlation precisely, we can again test whether the observed distribution is consistent with being random. The presence of 1 out of 7 LBGs from our  $I_{AB} \leq 25.5$  sample within  $15''$  of the QSO line-of-sight is inconsistent with a random distribution at the 95% confidence level.<sup>9</sup> Since G2 is not particularly close to the QSO or DLAs

in redshift this angular overdensity appears to be a coincidence rather than the projection of a three-dimensional structure.

## 7. DISCUSSION

We have not found significant evidence for autocorrelation amongst the 8 LBGs at  $z > 3.5$  in our current sample. It is therefore not surprising that we find no evidence for a cross-correlation between LBGs and damped Lyman  $\alpha$  absorbers, as the latter should be more difficult to detect if the DLAs are indeed less massive than the LBGs. Our results at  $z \simeq 4$  are comparable to the limited studies of the clustering environment of damped Lyman  $\alpha$  systems that have been performed at  $z \simeq 3$ . Steidel et al. (1996) found only one out of eleven Lyman-break galaxies in the field of Q0000-263 to be within  $\Delta z = 0.04$  of the  $z = 3.39$  DLA. Ellison et al. (2000) found two out of 27 LBGs in the field containing Q0201+1120 to be within  $\Delta z = 0.02$  of the  $z = 3.39$  DLA. This failure to detect clustering of LBGs with DLAs at  $z \simeq 3$  stands in contrast to the detection of strong autocorrelation of LBGs at  $z \simeq 3$  (Adelberger et al. 1998), although the latter was determined from a much larger sample of galaxies.

In order to obtain better statistics in the future, we have begun a systematic survey for Lyman-break galaxies associated with damped Lyman  $\alpha$  absorbers at  $z \simeq 3$ . The increased sky density of LBGs bright enough for spectroscopic identification at  $z \simeq 3$  and reduced sky noise near 5000 Å should allow us to obtain significantly improved statistics. The coincidence of LBG overdensity and damped Lyman  $\alpha$  redshifts in a number of fields would argue in favor of strong biasing and hence large mass of the damped Lyman  $\alpha$  absorbers, which is counter to the predictions of the  $\Lambda$ CDM model.

We see no positive indication of clustering of LBGs with the quasar BR 0951-04, but this quasar is at too high a redshift for us to be sensitive to an LBG-quasar cross-correlation except in the unlikely case that our expected redshift distribution is uniform. Observing fields with a quasar at lower redshift will allow us to measure the cross-correlation of quasars and LBGs, which will test the belief that quasars are highly biased markers of protoclusters (Djorgovski 1997). With better statistics, this observational program will measure the bias of DLAs, quasars, and Lyman-break galaxies, revealing much about the typical mass and environment of these high-redshift objects.

We wish to thank Kurt Adelberger, Chuck Steidel, and Dan Stern for invaluable conversations and Jeff Newman, Andy Bunker, Max Pettini, and the referee for their comments which improved this paper. We thank the Keck Observatory staff for their patient and skillful assistance with the observations. We used the BOGUS package written by Dan Stern, Andy Bunker, and Adam Stanford and cosmic ray removal routines written by Mark Dickinson to reduce our multislit data. AMW was partially supported by NSF grant AST 0071257, and JXP acknowledges support from a Carnegie postdoctoral fellowship.

<sup>8</sup>Because this bin centered at  $z = 3.71$  is below the mean redshift, the result is more significant for the gaussian expected redshift distributions, but this could easily be weakened if the true mean of the expected redshift distribution is  $z = 3.8$ . We will revisit this issue when the expected redshift distribution is better determined by observations in additional fields.

<sup>9</sup>G1 was selected only because it lies within  $10''$  of the quasar and was therefore excluded from this analysis.

## REFERENCES

Adelberger, K. L., Steidel, C. C., Giavalisco, M., Dickinson, M., Pettini, M., & Kellogg, M. 1998, *Astrophys. J.*, 505, 18

Bertin, E. & Arnouts, S. 1996, *Astron. Astrophys. Suppl. Ser.*, 117, 393

Bunker, A. J., Warren, S. J., Clements, D. L., Williger, G. M., & Hewett, P. C. 1999, *Mon. Not. R. Astron. Soc.*, 309, 875

Djorgovski, S. G. 1997, in *Structure and Evolution of the Intergalactic Medium from QSO Absorption Line Systems*, eds. P. Petitjean & S. Charlot, 303

Ellison, S. L., Pettini, M., Steidel, C. C., & Shapley, A. E. 2000, *Astrophys. J.*, in press, astro-ph/0010427

Fukugita, M., Ichikawa, T., Gunn, J. E., Doi, M., Shimasaku, K., & Schneider, D. P. 1996, *Astron. J.*, 111, 1748

Haehnelt, M. G., Steinmetz, M., & Rauch, M. 1998, *Astrophys. J.*, 495, 647

—. 2000, *Astrophys. J.*, 534, 594

Hogg, D. W. et al. 1998, *Astron. J.*, 115, 1418

Kauffmann, G. 1996, *Mon. Not. R. Astron. Soc.*, 281, 475

Lowenthal, J. D., Koo, D. C., Guzman, R., Gallego, J., Phillips, A. C., Faber, S. M., Vogt, N. P., Illingworth, G. D., & Gronwall, C. 1997, *Astrophys. J.*, 481, 673

Maller, A. H., Prochaska, J. X., Somerville, R. S., & Primack, J. R. 2000, preprint, astro-ph/0002449

Mo, H. J., Jing, Y. P., & White, S. D. M. 1996, *Mon. Not. R. Astron. Soc.*, 282, 1096

Mo, H. J., Peacock, J. A., & Xia, X. Y. 1993, *Mon. Not. R. Astron. Soc.*, 260, 121

Oke, J. B. et al. 1995, *Publ. Astron. Soc. Pac.*, 107, 375

Prochaska, J. X. & Wolfe, A. M. 1997, *Astrophys. J.*, 487, 73

—. 1998, *Astrophys. J.*, 507, 113

—. 1999, *Astrophys. J. Suppl. Ser.*, 121, 369

Steidel, C. C., Adelberger, K. L., Giavalisco, M., Dickinson, M., & Pettini, M. 1999, *Astrophys. J.*, 519, 1

Steidel, C. C., Giavalisco, M., Pettini, M., Dickinson, M., & Adelberger, K. L. 1996, *Astrophys. J. Lett.*, 462, L17

Steidel, C. C., Pettini, M., & Adelberger, K. L. 2000, preprint, astro-ph/0008283

Steidel, C. C., Pettini, M., & Hamilton, D. 1995, *Astron. J.*, 110, 2519

Storrie-Lombardi, L. J., McMahon, R. G., Irwin, M. J., & Hazard, C. 1996, *Astrophys. J.*, 468, 121

Storrie-Lombardi, L. J. & Wolfe, A. M. 2000, *Astrophys. J.*, 543, 552

Wolfe, A. M. 1993, *Astrophys. J.*, 402, 411

Wolfe, A. M. 1997, in *Structure and Evolution of the Intergalactic Medium from QSO Absorption Line Systems*, eds. P. Petitjean & S. Charlot, 243

Wolfe, A. M., Lanzetta, K. M., Foltz, C. B., & Chaffee, F. H. 1995, *Astrophys. J.*, 454, 698

Wolfe, A. M. & Prochaska, J. X. 2000a, *Astrophys. J.*, 545, 591

—. 2000b, *Astrophys. J.*, 545, 603

Wolfe, A. M., Turnshek, D. A., Smith, H. E., & Cohen, R. D. 1986, *Astrophys. J. Suppl. Ser.*, 61, 249

Yahata, N., Lanzetta, K. M., Chen, H., Fernández-Soto, A., Pascarelle, S. M., Yahil, A., & Puetter, R. C. 2000, *Astrophys. J.*, 538, 493

Zabludoff, A. I., Zaritsky, D., Lin, H., Tucker, D., Hashimoto, Y., Shectman, S. A., Oemler, A., & Kirshner, R. P. 1996, *Astrophys. J.*, 466, 104

TABLE 1  
OBSERVING LOG FOR IMAGING AND SPECTROSCOPY IN THE FIELD OF BR 0951–04.

Date	Observing Mode	Exposure Time (s)	Seeing (")	1 $\sigma$ sky AB <sup>a</sup> mag/sq. "	3 $\sigma$ source detection AB mag/FWHM <sup>2</sup>
1999 January 13	B imaging	4500	0.85	29.7	28.7
	R imaging	1620	0.75	29.0	28.1
	I imaging	1560	0.63	28.1	27.4
1999 March 22	longslit	7200	1.2		
1999 December 6	multislit-left	7200	1.0		
	multislit-right	3600	1.3		
2000 March 9	multislit-left	3600	1.1		
	multislit-right	7200	1.2		

<sup>a</sup> An AB magnitude of zero corresponds to  $3.64 \times 10^{-23}$  W m<sup>-2</sup> Hz<sup>-1</sup>. AB<sub>95</sub> magnitudes (Fukugita et al. 1996) can be converted to the Johnson-Cousins system using  $B_{JC} = B_{AB} + 0.15$ ,  $R_{JC} = R_{AB} - 0.18$ , and  $I_{JC} = I_{AB} - 0.43$ .

TABLE 2  
SPECTROSCOPIC RESULTS FOR CANDIDATE  $z > 3.5$  GALAXIES.

Category:	I	II	III	IV	V	all
$z > 3.5$	3	1	3	0	1	8
$z < 3.5$	3	6	3	1	0	13
uncertain	8	1	4	1	0	14
not observed	5	0	5	0	0	10
Total	19	8	15	2	1	45

I: meets two-color criteria,  $I_{AB} \leq 25$

II: selected based on photometric redshift,  $I_{AB} \leq 25$

III: meets two-color criteria,  $25 < I_{AB} \leq 25.5$

IV: selected based on photometric redshift,  $25 < I_{AB} \leq 25.5$

V: within  $10''$  of quasar,  $25.5 < I_{AB} \leq 26.0$

TABLE 3  
SPECTROSCOPICALLY CONFIRMED  $z > 3.5$  GALAXIES.

Galaxy:	z	$\sigma_z^a$	$I_{AB}$	$(B-R)_{AB}$	$(R-I)_{AB}$	$z_{prob}^b$	$z_{phot}^c$
G1	3.69	-0.05	25.7	2.2	0.0	0.74	3.78
G2	3.81	0.01	24.6	2.8	0.0	1.00	3.82
G3	3.72	+0.03	24.2	2.8	0.0	1.00	3.85
G4	3.57	0.01	24.8	1.6 <sup>d</sup>	-0.2	0.82	3.62
G5	3.75	+0.05	25.3	2.6	-0.1	0.91	3.76
G6	4.41	0.01	24.9	3.2	0.0	0.99	3.93
G7	3.72	0.01	25.2	2.3	-0.2	1.00	3.71
G8	4.14	+0.09	25.5	3.6	0.2	0.90	4.08

<sup>a</sup> A plus or minus sign indicates that a specific other redshift,  $z + \sigma_z$  is also a good fit. Otherwise, the errors are approximately symmetrical and roughly correspond to 95% confidence.

<sup>b</sup> Defined as the integrated probability that the redshift is in the range  $3.5 < z < 4.5$ . The method corresponds to assuming a uniform prior as a function of redshift but then optimizing the likelihood at each redshift over a set of possible template spectra.

<sup>c</sup> The redshift which maximizes the photometric redshift likelihood function.

<sup>d</sup> G4 falls outside of the color selection region and was included on the basis of its photometric redshift. The very blue  $R - I$  color makes it fall directly on the evolutionary track of starburst galaxies at  $z \simeq 3.6$  which are at too low redshift to drop out of the  $B$  filter as fully as the color criteria require.

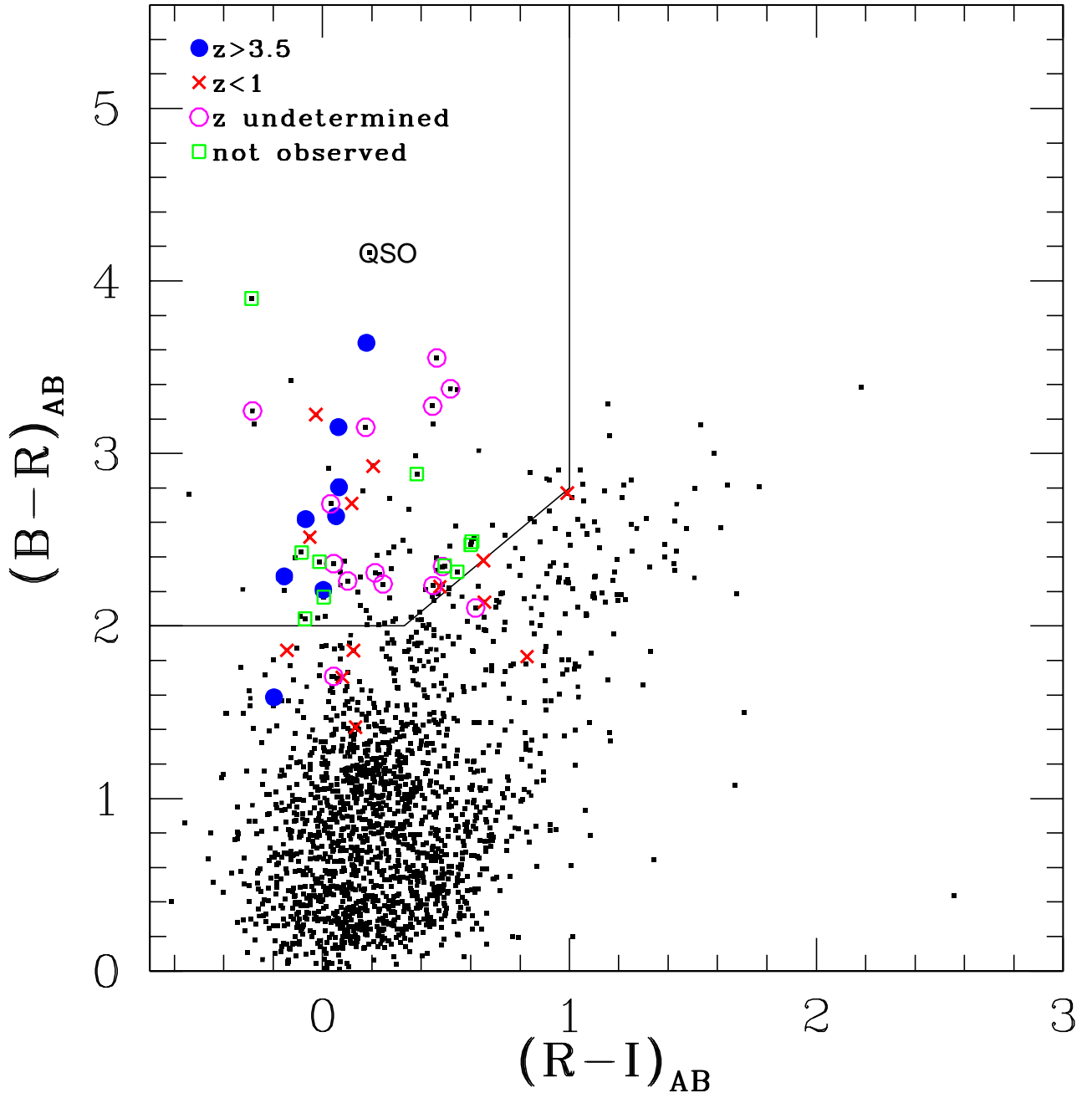


FIG. 1.— Two-color diagram of objects imaged in field of BR 0951–04 with  $I_{AB} \leq 25.5$  (with the addition of object G1). Objects that were selected as candidate LBGs based on their colors and/or photometric redshifts have been assigned large symbols as identified in the upper left corner. Objects that fall in the color selection region but are represented only by small points were found by visual inspection to have suspect photometry and were therefore not considered as candidate LBGs.

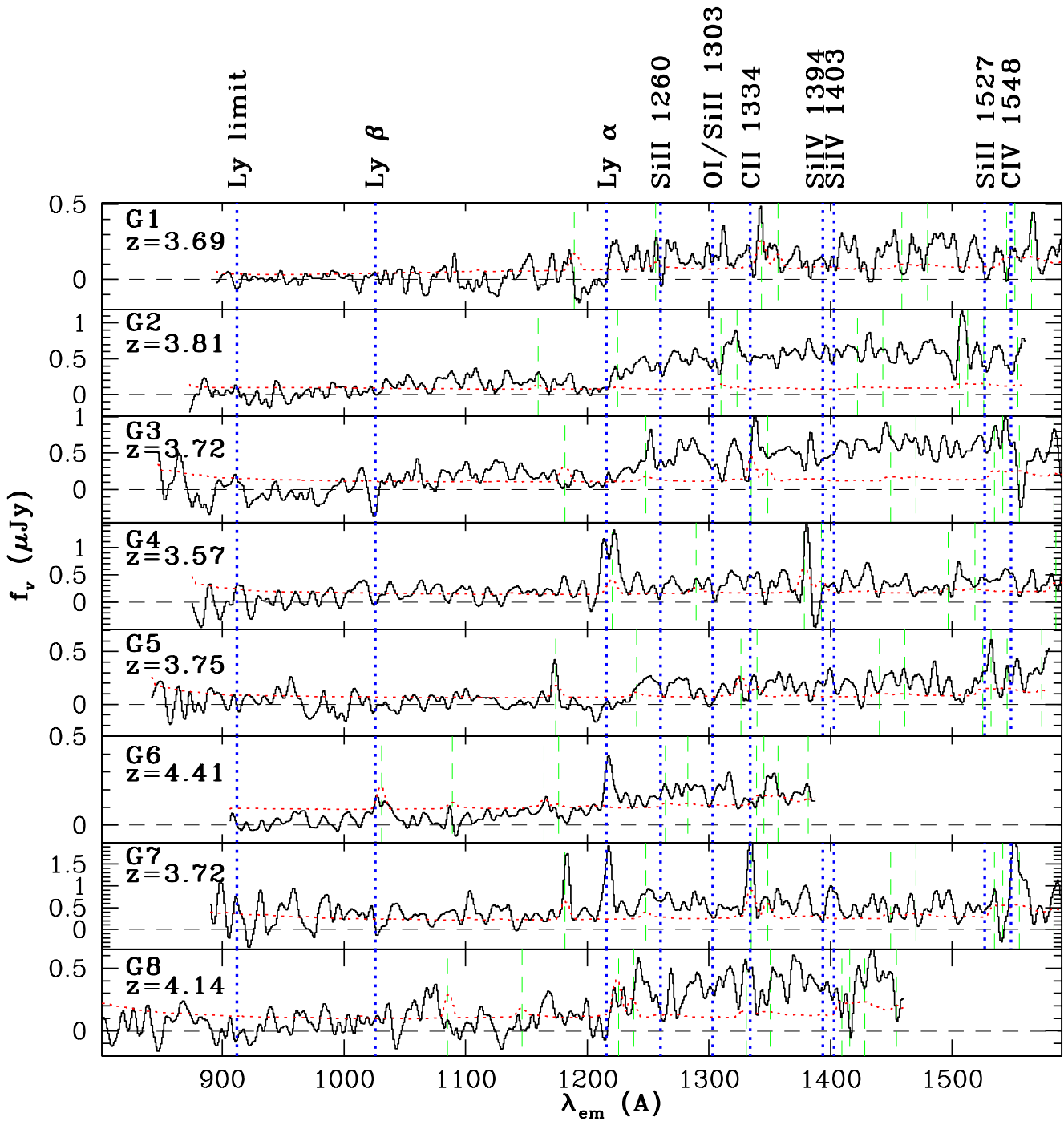


FIG. 2.— Spectra of 8 confirmed  $z > 3.5$  galaxies in the field of BR 0951–04 after being smoothed by the resolution element. The dotted spectrum shows the  $1\sigma$  uncertainty. Spectra are plotted versus inferred rest-frame wavelength, with dotted vertical lines showing expected absorption/emission features. Flux is shown in units of  $\mu\text{Jy}$  ( $1\mu\text{Jy} = 10^{-29} \text{ erg cm}^{-1} \text{ s}^{-1} \text{ Hz}^{-1}$ ). Dashed vertical lines show sky lines (at 5577, 5892, 6300, 6364, 6840, 6940, 7244, 7276, 7340, and 7475 Å) that are too strong to be subtracted well and can be used as a rough guide to the observed wavelengths. Observed wavelengths from 4000 to 7500 Å are shown; the signal-to-noise degrades considerably below that due to reduced grating throughput and CCD quantum efficiency and above that due to sky emission bands. Object G6 was observed with a GG495 dichroic, so only wavelengths above 4900 Å are shown.

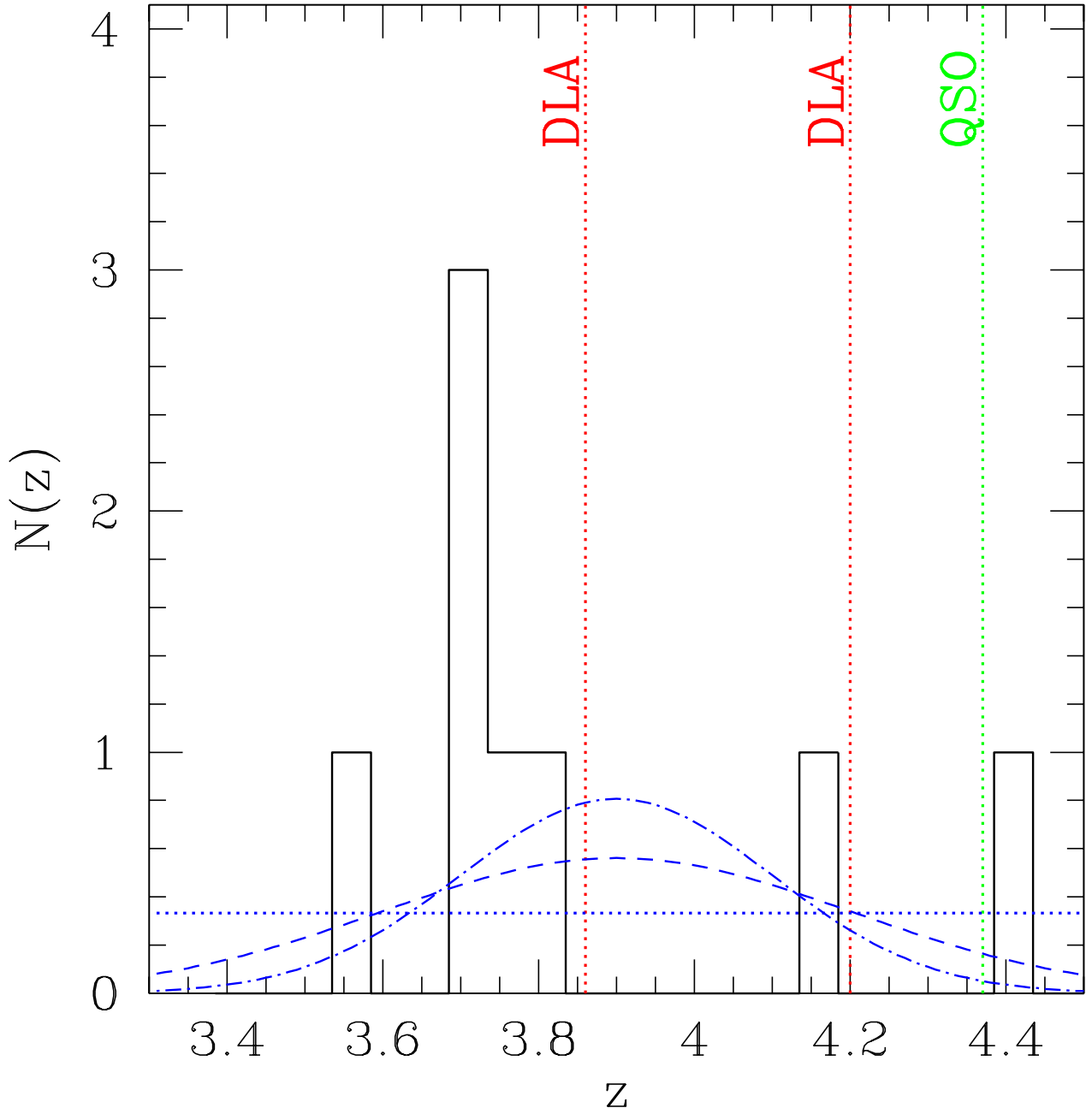


FIG. 3.— Histogram of redshifts of LBGs in field of BR 0951–04. Redshifts of DLAs and quasar are shown by vertical dotted lines. The range of possible expected redshift distributions described in the text is also plotted; the dot-dashed line has mean  $z = 3.9$ ,  $\sigma = 0.2$ , the dashed line has mean  $z = 3.9$ ,  $\sigma = 0.3$ , and the dotted line is a uniform distribution from  $z = 3.3$  to  $z = 4.5$ . All are normalized to produce 8 galaxies.